Chapter

Flood Damage Reduction in Land Subsidence Areas by Groundwater Management

Yin-Lung Chang, Jinn-Chuang Yang, Yeou-Koung Tung, Che-Hao Chang and Tung-Lin Tsai

Abstract

Continuing land subsidence can diminish the effectiveness of an existing flood mitigation system and aggravate the flood hazard. This chapter demonstrates that, through groundwater management with an effective pumping scheme, flood hazard and related flood damage in land subsidence area can be reduced. The chosen study area is in the southwest coast of Taiwan, which has long been suffering from frequent and wide-spread flooding primarily due to land subsidence induced by groundwater overpumping. Numerical investigation in the study area clearly shows that effective management of groundwater pumping can play an important role in long-term sustainable solution for controlling the spatial-temporal variability of future land subsidence, preventing the flood hazard from worsening, reducing the flood damage, and satisfying the groundwater demand.

Keywords: flood hazard, flood damage reduction, risk analysis, groundwater management, land subsidence

1. Introduction

In the region with scarce or highly variable surface water resource, groundwater is a vitally important source of water for sustainable development of the region. Groundwater pumping without proper control and management could result in a rapid depletion of valuable groundwater resource, which cannot be replenished in a short period of time. Furthermore, the seriousness of land subsidence can be exacerbated, which is concomitant with increased flood hazard and damage. Phien-wej et al. [1] reported that the estimated flood damage attributed to land subsidence in the 1990s amounted to $12 million annually in Bangkok, Thailand. Nicholls et al. [2], in their assessment of the exposure of population and assets to a 1-in-100 year surge-induced flood event at 136 port cities with more than one million inhabitants, indicated that the climate change and land subsidence contribute about one-third of increased flood exposure for people and assets. The impact of land subsidence induced by excessive groundwater extraction should be carefully examined in deltaic cities, especially in those coastal areas that are under rapid development.

By using inundation models, many studies have shown that flood hazard, after a long period of land subsidence, becomes worsened in cities like Semarang [3] and Jakarta [4] of Indonesia, Shanghai of China [5], and coastal cities around Northern

Adriatic Sea [6]. All the above studies showed that land subsidence results in increased flood inundation depth and areal extent, as well as diminishing effectiveness of existing flood protection systems. Even the flood defense system is upgraded to uphold the protection level, and the flood risk will be worsening with continuing land subsidence. Therefore, an engineered flood defense infrastructure system, jointly with a proper groundwater pumping practice with an aim to reduce land subsidence, could offer a sustainable solution to flood management problems in subsidence prone areas.

The goal for land subsidence mitigation can be achieved through effective management of groundwater pumping by constraining the drawdown. A comprehensive review of groundwater management (GWM) can be found elsewhere [7–9]. The common approach for handling subsidence control in GWM is to set a preconsolidation head as the lower bound of the groundwater level to prevent inelastic soil compaction from happening [10]. However, such an approach considers only the drawdown constraint that does not explicitly relate to the magnitude of land subsidence. To circumvent such deficiency, Chang et al. [11, 12] developed a mixed integer programming model for maximizing total pumpage, subject to drawdown and land subsidence constraints. 1D consolidation equation, which simultaneously considers inelastic and elastic soil compaction, is incorporated explicitly in the subsidence constraints.

As many studies have pointed out that the flood risk in land subsidence prone areas can be reduced through proper GWM (e.g., [1, 5]), and it is rarely found that flooding is explicitly incorporated into the model formulation. Chang et al. [13] developed a groundwater pumping optimization model, in conjunction with land subsidence and inundation models, to mitigate the land subsidence effect on flood hazard in land subsidence areas and satisfy the water demand. The GWM model determines the optimal pumping scheme for (1) minimizing land subsidence, (2) preventing flood hazard from worsening in the future, and (3) satisfying groundwater demand. This chapter, on the basis of the developed optimal groundwater pumping model [13], evaluates flood damage reduction and assesses economic benefit attainable by GWM in land subsidence prone coastal areas.

2. Methodology

2.1 Analysis framework

Figure 1 shows the framework of analysis that was applied to a study area in the coastal zone of Taiwan (see Section 3.1 for more detailed descriptions) that is experiencing severe land subsidence problem largely due to groundwater overpumping. It can be seen that the analysis framework contains two major parts in which the first part is on the left branch for predicting the cumulative land subsidence in the study area over a 10-year period (2012–2021) based on the existing groundwater usage without management. Under this scenario, the groundwater pumpage in 2012–2014 in the study area was set to the historical average value as shown in **Table 1**. In 2015, a newly built Hushan reservoir began its service, and the groundwater pumpage during 2015–2021 was adjusted downward according to the planned water supply amount from the reservoir. The left branch of the analysis estimates the ground surface topography in the study area caused by land subsidence after 10 years of using the existing pumping pattern without optimal GWM. Flood hazard and inundation damage in the study area at the end of 2021 are assessed accordingly.

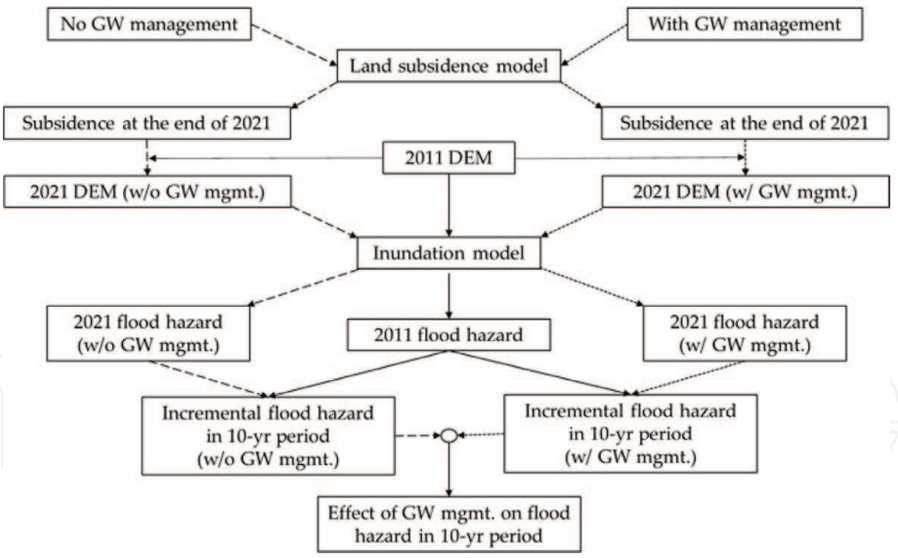

Figure 1.
Flow chart showing the methodological framework in the study.

Township	Area (km^2)	Extraction		Recharge	
		Annual (10^6 m^3)	Intensity (mm/day)	Annual (10^6 m^3)	Intensity (mm/day)
Mailiao	80.17	107.55	3.68	27.25	0.93
Lunbei	58.48	115.89	5.43	7.46	0.35
Taisi	54.10	34.4	1.74	17.13	0.87
Dongshih	48.36	57.33	3.25	7.54	0.43
Baojhong	37.06	54.05	4.00	8.22	0.61
Tuku	49.02	56.6	3.16	6.39	0.36
Huwei	68.74	85.18	3.39	15.25	0.61
Sihhu	77.12	58.26	2.07	25.42	0.90
Yuanchang	71.59	89.01	3.41	9.93	0.38
Total	464.47	658.27	30.13	124.59	5.44

Table 1.
Groundwater extraction and natural recharge for the nine townships in the study area.

It should be pointed out here that, because of a relatively short management period of 10 years considered in the study, the rainfall condition was assumed to be stationary in assessing flood hazard and inundation damage. The indicators of flood hazard considered include the levee freeboard along the drainage channel systems and the maximum inundation depth in the study area. The freeboard is a measure of margin of safety, which is the vertical elevation difference from the levee crown to the water surface in the drainage channel. A reduction in the freeboard is an indication of increased overtopping potential of the levee system. The maximum inundation depth can be indicative of flooding severity. From the flood inundation simulation, the effect of subsidence on the flood hazard under the existing groundwater pumping practice can be assessed. With flood damage-inundation depth relationships available, the flood inundation risk cost can be assessed.

The second part of the analysis is shown on the right-hand branch of **Figure 1** in which the GWM model is applied to find the optimal pumping scheme by

minimizing the land subsidence effect on flood hazard while, at the same time, satisfying the water demand. After obtaining the optimal pumping strategy, the corresponding land subsidence amounts are obtained to define the land topography in Year 2021. Under a different topography, the corresponding flood hazard indicators and inundation damage are obtained for assessing the effect of GWM.

2.2 Inundation and land subsidence models

2.2.1 Inundation model

The well-known SOBEK Suite [14], developed by the Deltares Research Institute in the Netherlands, was used in the study to model flood inundation and the associated hazard. Specifically, the hydrodynamic module, which contains 1D-flow and 2D-overland flow submodules, was used to simulate surface water flow in the study area for determining the levee freeboard and inundation depth under the selected design rainfall events.

The major inputs to the SOBEK 1D/2D simulation for this study are as follows:

1. *Rainfall hyetograph*: 24-hour design rainfall with six design frequencies (i.e., 2-, 5-, 10-, 25-, 50-, and 100-year) was used. Their corresponding rainfall amounts were 158, 227, 275, 337, 384, and 432 mm, respectively. All six design storm events follow the same dimensionless rainfall pattern as shown in **Figure 2** [15]. For simplicity, no spatial variation of rainfall in the study area was considered.

2. *Downstream boundary*: since major drainage lines in the study area are connected to the Taiwan Strait, the boundary condition at the downstream end sections was assigned with a wave form shown as the dash line in **Figure 2**.

3. *Channel profile and DEM*: the cross-sectional profile along the drainage lines and DEM within the study area were surveyed in 2012. By considering the trade-off between the accuracy and computational efficiency of hydrodynamic simulation, the grid for the 2D overland flow simulation was set to 120 m. To simulate flood hazard with the projected land subsidence in 2021, the ground

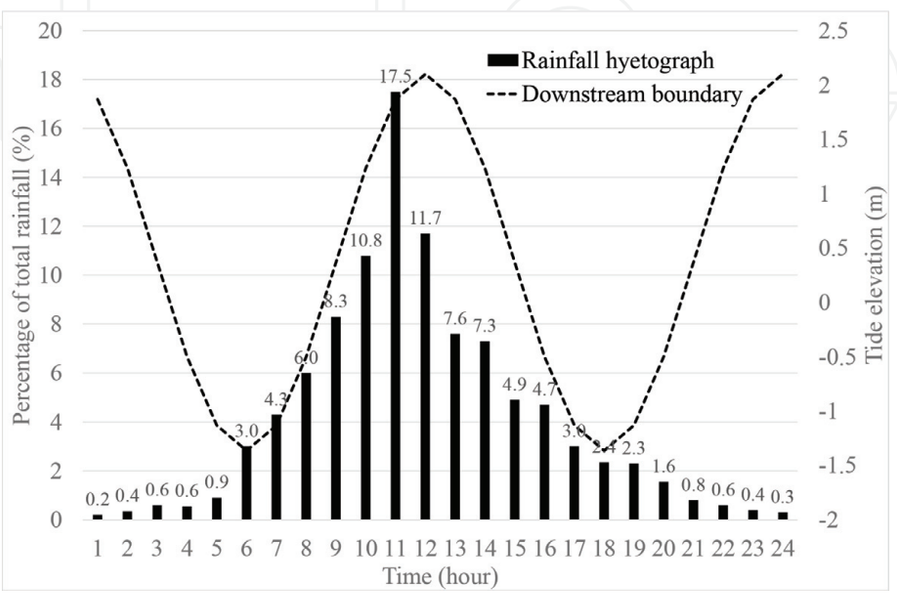

Figure 2.
Dimensionless 24-hr design rainfall hyetograph and the downstream tide level for boundary condition [15].

elevation in 2012 was added by the cumulative land subsidence between 2012 and 2021 obtained by the land subsidence model under the conditions of with and without GWM.

4. *Roughness coefficient*: flow boundary roughness is categorized by the channel bed and overland surface. As almost all the drainage channels within the study area are man-made with gravel bottom and concrete siding, the nominal value of 0.02 for the Manning roughness coefficient was used according to Chow [16]. The roughness coefficient of the overland surface was determined by the land use listed in **Table 2**.

2.2.2 Land subsidence model

In this study, land subsidence is assumed to be caused by groundwater pumping. An uncoupled model consisting of a layered 3D groundwater solver and a 1D consolidation model was used to simulate land subsidence [17]. The layered 3D groundwater solver is first used to simulate depth-averaged groundwater flow and pore pressure head change due to groundwater extraction in every layer at each time step. The vertical soil displacement during each time step is then calculated by the 1D consolidation equation. The simulation model assumes (1) isotropic soil medium, (2) linear elasticity relationship between average effective stress and average displacement following Hooke's law, and (3) vertical displacements only. These assumptions, however, ignore the presence of the preconsolidation head, which implies that a decrease in pore pressure head due to groundwater extraction will always cause normal consolidation and is unable to consider overconsolidation and rebound (i.e., elastic range). This renders overestimation of land subsidence.

To simultaneously consider the inelastic/elastic behavior of land subsidence, Chang et al. [12] modified the 1D consolidation equation according to Leake [18] as

$$\Delta s_{l,k,t} = \begin{cases} \alpha C_c\left(\Delta h^{p}_{l,k,t-1} - \Delta h_{l,k,t-1}\right) + C_c\left(\Delta h_{l,k,t} - \Delta h^{p}_{l,k,t-1}\right), \Delta h_{l,k,t} > \Delta h^{p}_{l,k,t-1} \\ \alpha C_c\left(\Delta h_{l,k,t} - \Delta h^{p}_{l,k,t-1}\right), \Delta h_{l,k,t} \le \Delta h^{p}_{l,k,t-1} \end{cases} \tag{1}$$

$$\Delta \mathrm{h}^{\mathrm{p}}_{\mathrm{l,k,t}} = \mathrm{Max}\left[\Delta \mathrm{h}_{\mathrm{l,k,t}}, \Delta \mathrm{h}^{\mathrm{p}}_{\mathrm{l,k,t-1}}\right] \tag{2}$$

where $\Delta s_{l,k,t}$ = land subsidence within layer-l at control point-k during the t-th time period; $\Delta h_{l,k,t}$ = drawdowns of layer-l at control point-k at the end of the t-th time period; α ($<<1$) = ratio of elastic to inelastic compaction per unit increase in drawdown; $C_c = \rho_u g B/(2\,\mu + \lambda)$ with ρ_w = density of water, g = gravitation

Land use	***kn***
Agriculture	0.8
Built-up	10
Water conservation	0.2
Amusement and rest area	3
Transportation	1
Other	0.5

Table 2.
Relationship between the Nikuradse roughness coefficient kn and land use [15].

acceleration, B = layer thickness, and μ, λ = Lame constants; and $\Delta h^{p}_{l,k,t}$ = difference between initial head and preconsolidation head at the end of the t-th time period. The positive value of $\Delta h^{p}_{l,k,t}$ denotes that the initial head is higher than the preconsolidation head. The total land subsidence amount at the control point-k can be determined by

$$\Delta s(k) = \sum_{l=1}^{NL} \sum_{t=1}^{NT} \Delta s_{l,k,t} \tag{3}$$

where NL, NT = the numbers of layer and time period, respectively. More detailed descriptions on the land subsidence model can be found in the studies of Chang et al. [11, 12].

In the process of developing the groundwater subsidence model for the study area, monitored data on pore pressure head and land subsidence during 2007–2009 were used to calibrate the model parameters such as hydraulic conductivity and soil compaction coefficients. Then, monitored data made in 2010–2011 were used for validation. The validated model was used to predict the cumulative land subsidence in the study area over a 10-year period during 2012–2021. Calibration and validation of pore pressure head and land subsidence in the study area were found quite satisfactory for pore water pressure and less satisfactory for land subsidence [13]. The reason might be because groundwater extraction alone is not the only cause for land subsidence. In addition, the 1D consolidation equation used in the land subsidence model cannot account for the body force and viscoelastic effects, which might have influences on land subsidence in thick aquitards. However, the validation results indicate that the simulation model can reasonably reproduce the general pattern of land subsidence in both time and space.

2.3 Optimal groundwater pumping model

Before developing a viable GWM for optimal pumping in the study area, insights were gained by applying the validated simulation model to examine the subsidence behavior under the existing pumping practice. The simulation results indicated that the levee freeboard and maximum inundation depth have a similar tendency in spatial variation affected by land subsidence. Both tend to become worsened in the near-shore low-lying area due to reduced difference between the sea level and levee crown elevation. Thus, continuing land subsidence would worsen the flood hazard in this area, and the results are consistent with those of Ward et al. [4] and Wang et al. [5]. On the other hand, outside the near-shore low-lying area, it was found that the freeboard and maximum inundation depth do not necessarily get worse. This is because the influence of the downstream boundary condition defined by the sea level is minimal. Instead, the relative variation of land subsidence in space becomes the dominant factor affecting the changes in freeboard and maximum inundation depth because it alters the slopes of drainage channels and the land surface.

By incorporating the above insights about land subsidence—flood hazard interrelationship, an effective GWM model can be developed for reducing the undesirable pumping-induced land subsidence and flood hazard in the study area. For the near-shore low-lying area, one could reduce the land subsidence amount because flood hazard is highly related to the magnitude of land subsidence. For the region outside the near-shore low-lying area, one could reduce the relative variation of land subsidence in space to prevent flood hazard from worsening. The optimal groundwater pumping model can be formulated as

$$\text{Minimize max } [\Delta s(k_{uc})]\ k_{uc} = 1, \ldots, NUC \tag{4}$$

$$\text{Subject to } \Delta s(k_c) \le \Delta s^*(k_c)\ k_c = 1, \ldots, NC \tag{5}$$

$$\sum_{j=1}^{NP} Q(j,t) \ge Q_D(t)\ t = 1, \ldots, NT \tag{6}$$

$$Q^L(j,t) \le Q(j,t) \le Q^U(j,t) \tag{7}$$

in which k_{uc} = the k_{uc}-th control point outside the near-shore low-lying area; k_c = the k_c-th control point within the near-shore low-lying area; NUC and NC = number of control points outside and inside the near-shore low-lying area, respectively; $\Delta s(\bullet)$, $\Delta s^*(\bullet)$ = cumulated and the maximum allowable land subsidence, respectively, at control points at the end of the management period; NP = number of pumping wells; $Q(j,t)$ = pumping rate at the j-th well during the t-th time period; $Q_D(t)$ = groundwater demand during the t-th time period; and $Q^L(j,t)$,$Q^U(j,t)$ = minimum and maximum allowable pumping rates, respectively, at the j-th well during the t-th time period.

The objective function Eq. (4) is to minimize the maximum land subsidence among all control points outside the near-shore low-lying area. The consideration of Eq. (4) can optimally reduce the magnitude and spatial variation of land subsidence outside the near-shore low-lying area. On the other hand, for any control point within the near-shore low-lying area, constraint Eq. (5) that directly limits the land subsidence can be imposed to prevent flood hazard from worsening due to the reduced levee freeboard.

3. Model application

To demonstrate the positive contribution of GWM to flood hazard reduction in land subsidence prone areas, the optimal groundwater pumping model developed by Chang et al. [13] is applied here to a selected study area in Taiwan.

3.1 Description of the study area

The study area chosen has a catchment area of 267 km^2 located in the northwest part of Yunlin County, Taiwan (see **Figure 3**). The northern boundary of the study area is defined by the Zhuoshui River, the longest river in Taiwan, and the western boundary is adjacent to the Taiwan Strait. The study area covers nine townships and has four drainage systems consisting of Shihtsoliao, Yutsailiao, Makungtso, and Chiuhuwei. The mean annual rainfall in the study area is about 1200 mm of which about 80% of rainfall occurs between May and September due to monsoons and typhoons (see **Table 3**). Despite the fact that the mean annual rainfall in the study area is less than half of the average value in Taiwan (i.e., 2500 mm), the study area is still highly susceptible to flood hazard due to its low lying and flat terrain.

Figure 4 is the topographic map of the study area, which shows its ground elevation ranging from −1.0 to 28 m with reference to the mean sea level. The east-to-west average land surface gradient is less than 1/1000 indicating that the surface runoff produced by heavy rainfall can be easily trapped in the study area. Furthermore, ground elevation in the downstream part of the study area is lower than the average spring high tide of 2.1 m. This implies that flood water in the drainage channels from a rainstorm event may not be effectively drained into the Taiwan Strait due to the backwater effect.

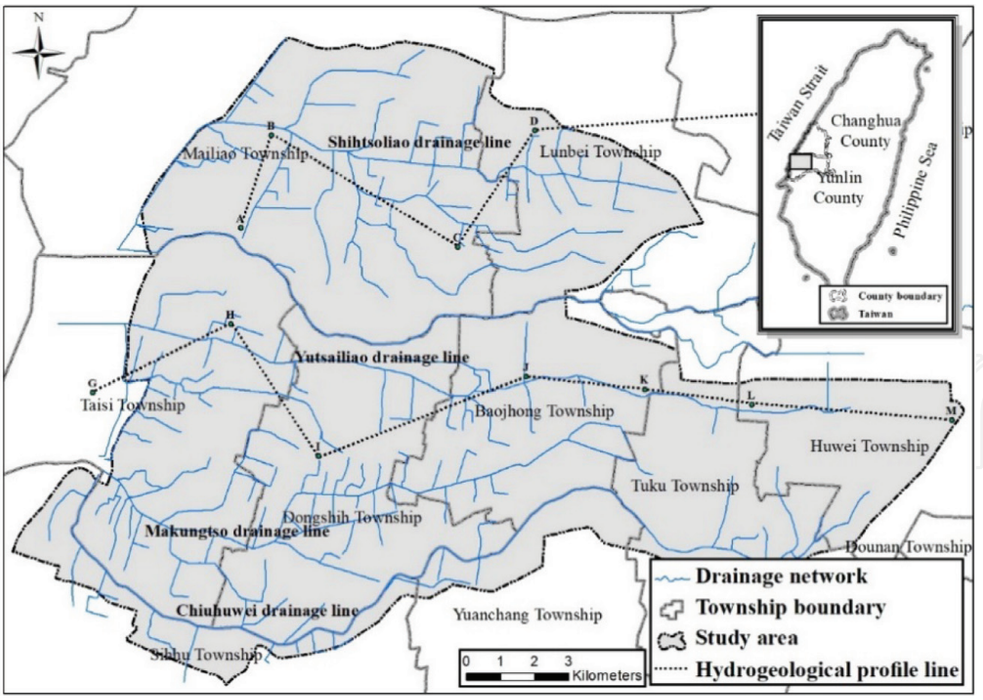

Figure 3.
Geographical location of the study area.

Month	Jan	Feb	Mar	Apr	May	Jun
Rainfall (mm)	19.6	35.2	50.3	78.2	159.3	269.5
Month	**Jul**	**Aug**	**Sept**	**Oct**	**Nov**	**Dec**
Rainfall (mm)	209.5	221.6	100.8	16.7	18.1	14.8
Annual Avg (mm)	1176.8					

Table 3.
Mean monthly rainfall amount in the study area.

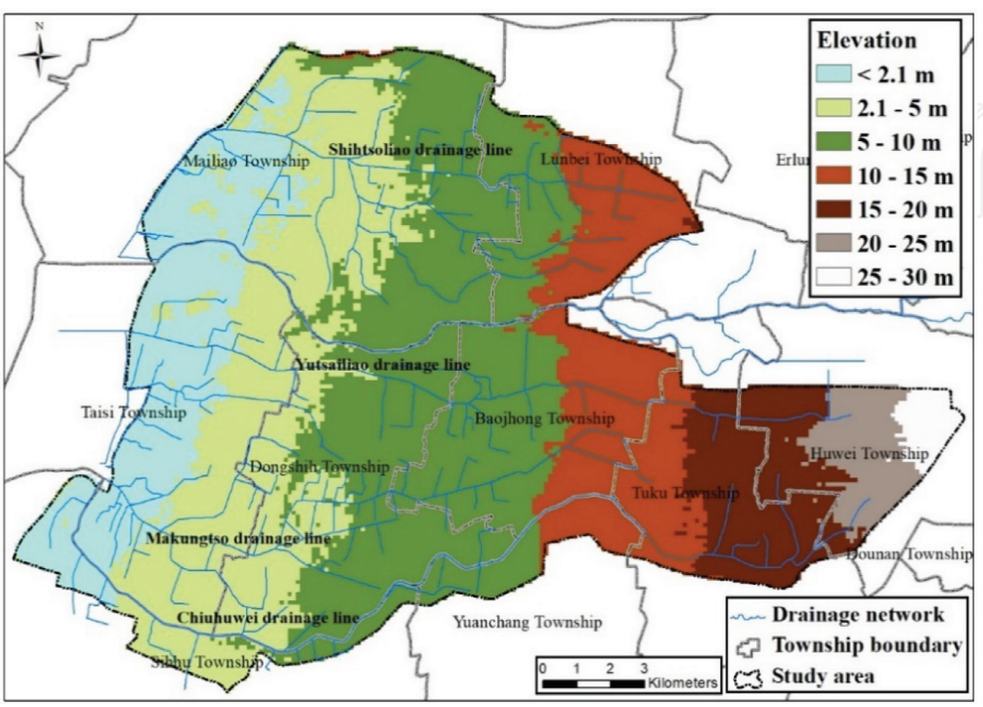

Figure 4.
Spatial distribution of ground elevation in the study area.

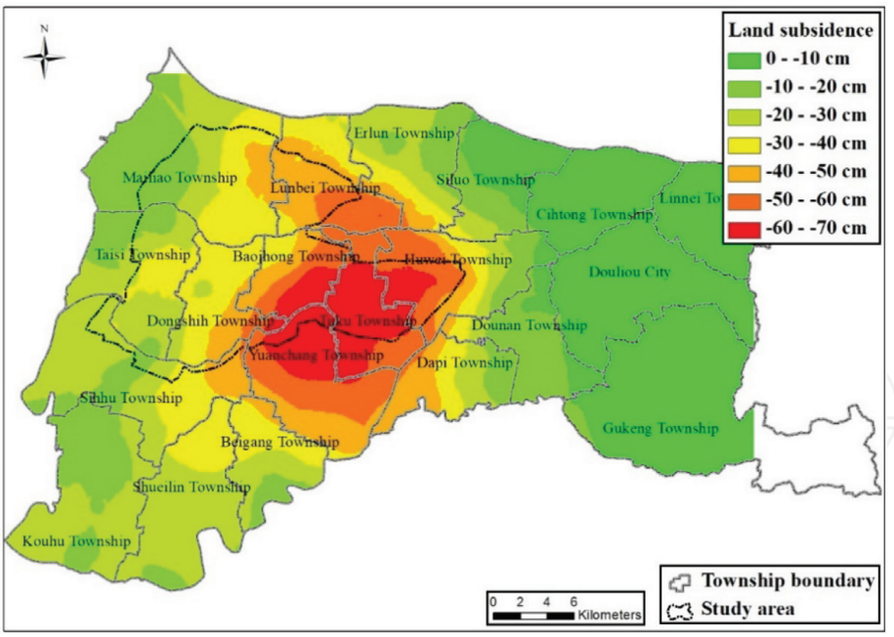

Figure 5.
Contour map of cumulative land subsidence in 2002–2011 in the study area.

Yunlin County is an important region for agriculture and freshwater fish farming in Taiwan. The two activities require a tremendous amount of fresh water, especially the latter. Due to the lack of sufficient and stable surface water supply in the area, groundwater pumping is widely used to secure fresh water. According to the record, groundwater constitutes 30% of agricultural water usage and almost 100% of domestic use in Yunlin County. **Table 1** lists the average groundwater extraction and recharge for the nine townships in the study area which shows that annual average groundwater extraction significantly exceeds the annual natural groundwater recharge. Since groundwater has been excessively pumped for more than 30 years in the general area of Yunlin County, serious land subsidence problem has been created. **Figure 5** shows the cumulative land subsidence during 2002–2011 in Yunlin County with negative values representing the ground elevation being lowered.

The study area is highly susceptible to flooding due to low lying and flat terrain. Progressive land subsidence further exacerbates flood hazard. To mitigate flood hazard in the area, the Water Resources Agency (WRA) of Taiwan had spent more than 3 billion $NT (approx. 0.1 billion $US) during 2006–2013 to strengthen and heighten the sea wall and levee of drainage channels, construct the polder protection system, and upgrade the pumping stations and tidal gates. Because groundwater extraction in the area was not effectively controlled and managed, the land subsidence continued to erode away the effectiveness of flood protection infrastructure systems with time.

3.2 Effect of optimal GWM on land subsidence and flood hazard

3.2.1 Land subsidence

After the optimal pumping strategy is obtained, the right-hand branch of the analysis framework (see **Figure 1**) is implemented to evaluate the effect of GWM. **Figure 6** shows the change in the land subsidence amount under the conditions of with and without GWM. A positive-valued change means that the land subsidence is reduced under the optimal pumping scheme. **Figure 6** indicates that, while satisfying the groundwater demand of each township, the optimum pumping

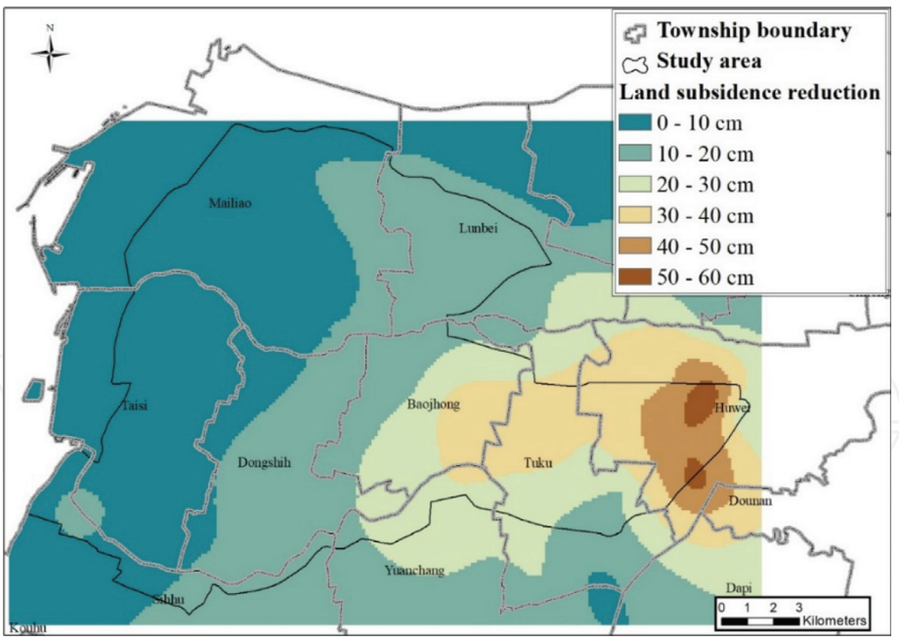

Figure 6.
Reduction in cumulative land subsidence due to GWM in the study area.

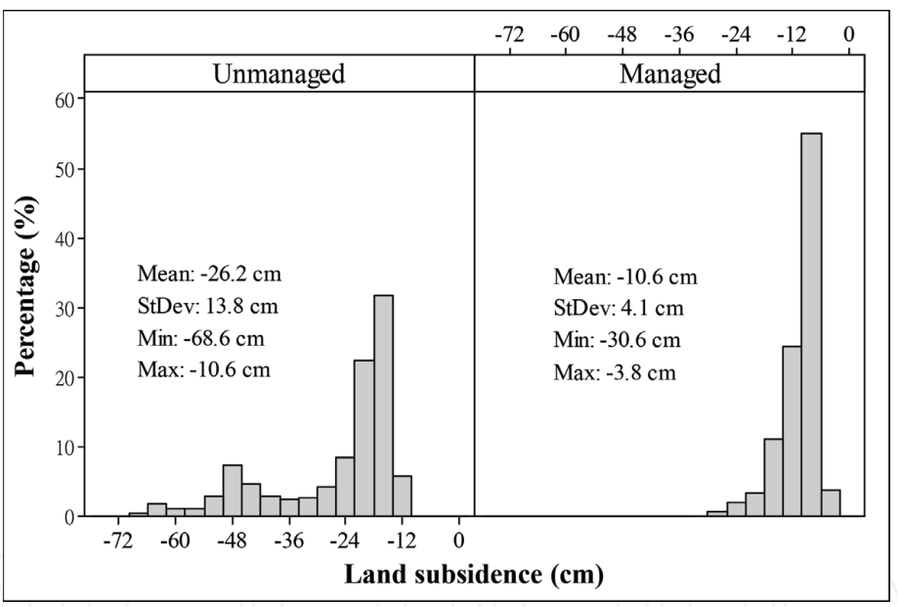

Figure 7.
Histograms of the cumulative land subsidence in 2012–2021 under the conditions of with and without GWM.

strategy could greatly reduce the land subsidence in the study area. The most reduction in land subsidence ranging from 40 to 60 cm occurs in Huwei and Tuku townships where the land subsidence was the most serious without GWM.

Figure 7 shows the histograms of cumulative land subsidence during 2012–2021 under the conditions of with and without GWM. Without GWM, the histogram on the left shows that the magnitude of land subsidence in the study area varies between −10 and −68 cm with the standard deviation of 13.8 cm. On the other hand, under the optimum pumping strategy, the histogram on the right shows that the range of land subsidence variation is greatly narrowed, and the standard deviation is reduced to 4.1 cm. Both **Figures 6** and **7** indicate that the magnitude and the spatial variation of land subsidence in the study area can be significantly reduced through optimum management of groundwater pumping.

3.2.2 Levee freeboard

Under the optimal GWM, **Figure 8** shows the change in the freeboard after a 10-year land subsidence where the study is subject to a 100-year design rainstorm. The solid black line in **Figure 8** is the contour of cumulative land subsidence over 2012–2021 with a contour interval of 2 cm. **Figure 9** further shows the histogram of the difference in the 2021 freeboard between the conditions of with and without GWM. The change with the positive value represents that the freeboard with GWM is greater than that without GWM when subject to a 100-year design rainfall. An

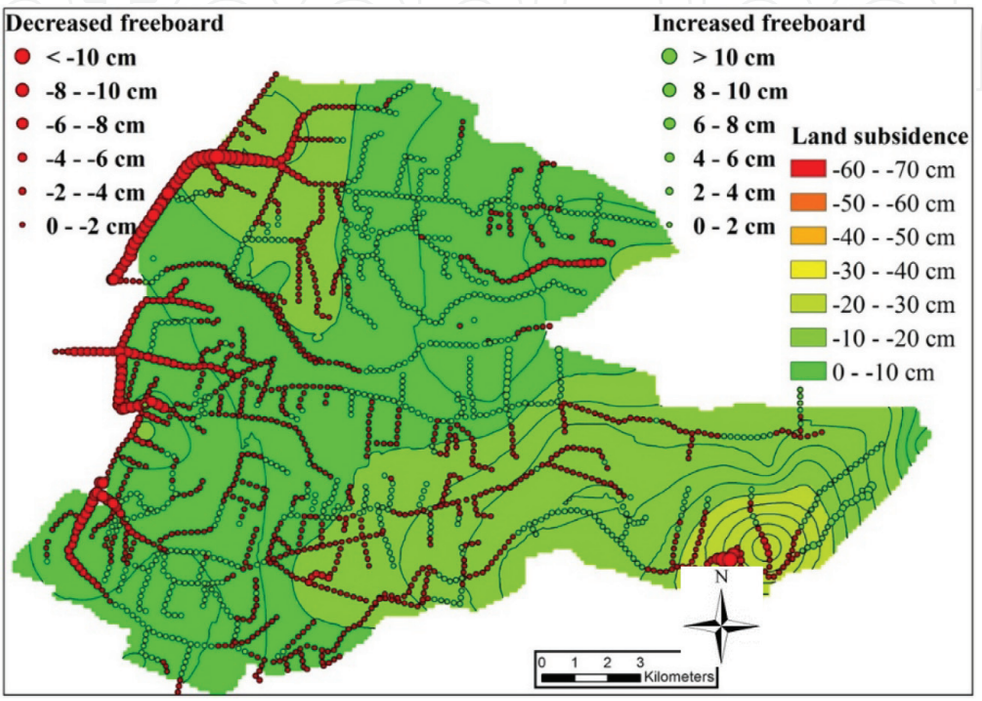

Figure 8.
Change in the levee freeboard after a 10-year land subsidence under the 100-year design rainstorm with GWM.

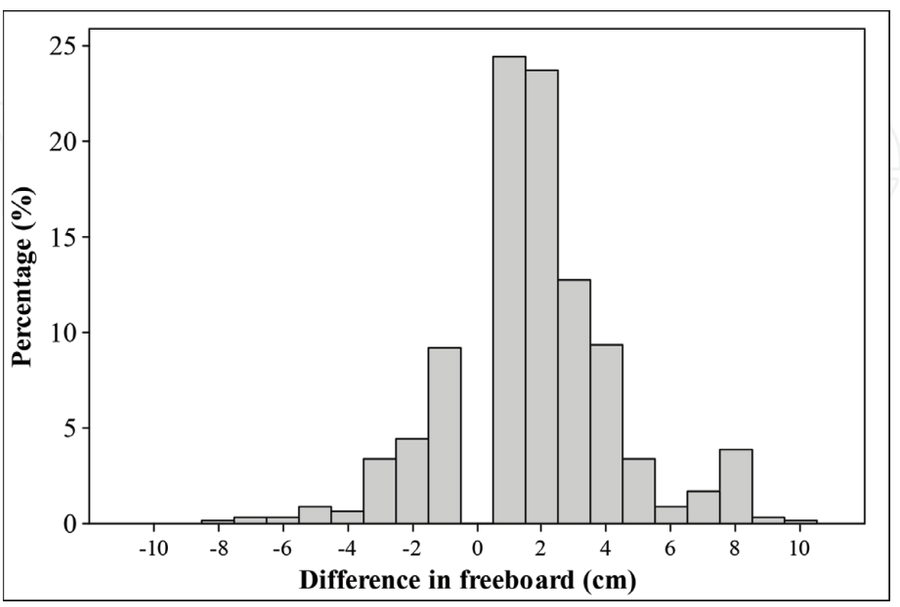

Figure 9.
Histogram of the difference of the levee freeboard in Year 2021 between conditions of with and without GWM under the 100-year design storm.

increase in the freeboard indicates overflow potential from drainage channel systems that is reduced through GWM. The most significant difference reaches 8–10 cm which occurs in the near-shore low-lying area (see **Figure 8**). The results clearly indicate that GWM can prevent the levee freeboard from decreasing and thereby sustain the effectiveness of the existing flood protection system over the management period. Even if it is required to upgrade the protection level in some areas, GWM can render a smaller scale for upgrading work and lower capital cost.

3.2.3 Maximum inundation depth

Figure 10 shows the difference in the maximum inundation depth in Year 2021 with and without GWM under the 100-year design rainstorm. The effect of GWM on the inundation depth is observed to be similar to that on the levee freeboard. It was found that the inundation depth in the near-shore low-lying area increases with 2021 land subsidence even with GWM. However, the range of increase is narrowed because the optimum pumping strategy greatly reduces the land subsidence in this area. The most reduction in inundation depth reaches 4–6 cm which occurs in the downstream of Yutsailiao and Chiuhuwei drainage lines (see **Figure 10**). The inundation depth could further be reduced if the maximum allowable land subsidence in Eq. (5) is set in a more restrictive manner. However, a more restrictive land subsidence control policy would result in a less amount of groundwater pumping which means that the current demand for the near-shore townships may not be satisfied.

Outside the near-shore low-lying area, the optimum pumping strategy can effectively prevent the inundation depth to be changed because of the reduced spatial variation of land subsidence. An exception is found at the farthest upstream from the Chiuhuwei drainage line where the inundated area grows larger with GWM because the land subsidence cone is moved to this area under the optimum pumping strategy. However, the gradient of land subsidence near this area under the condition of GWM is not as large as that of without GWM. Therefore, the increase in the inundated area would not greatly influence the flood hazard and the effectiveness of the existing flood protection system.

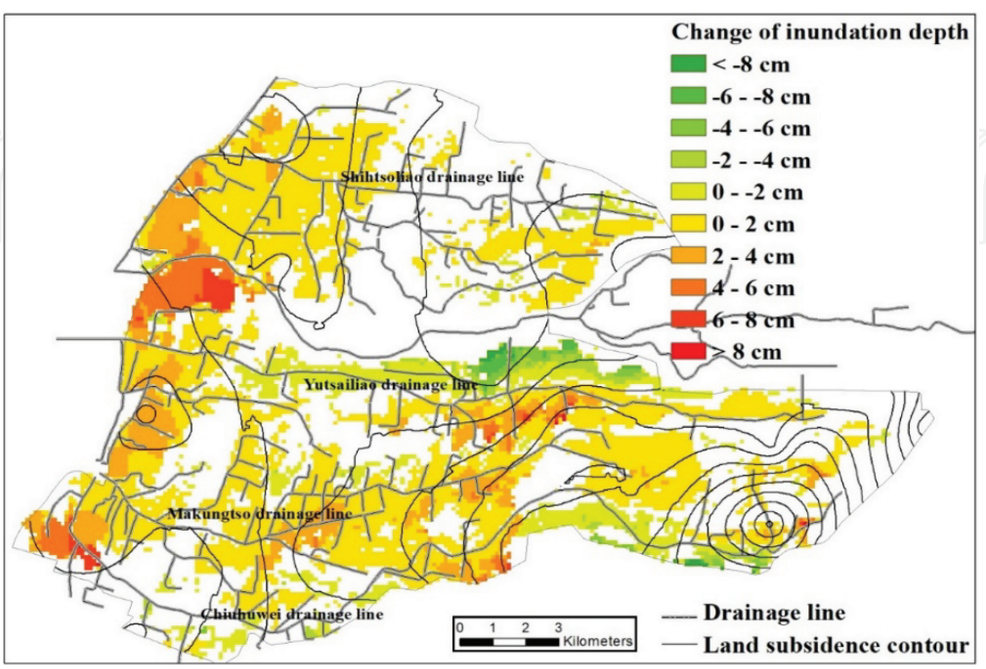

Figure 10.
Change in maximum inundation depth after a 10-year land subsidence with GWM under the 100-year design rainstorm.

3.2.4 Flood damage reduction

To assess land subsidence-induced flood risk cost in the study area, representative relationships between inundation area and flood damage for several economic crops, aquacultural produces, and buildings were established and are shown, respectively, in **Figures 11–13** according to past flood events. Then, by applying the flood inundation model on different land surface topographies in the study area under the conditions of with and without GWM and the design

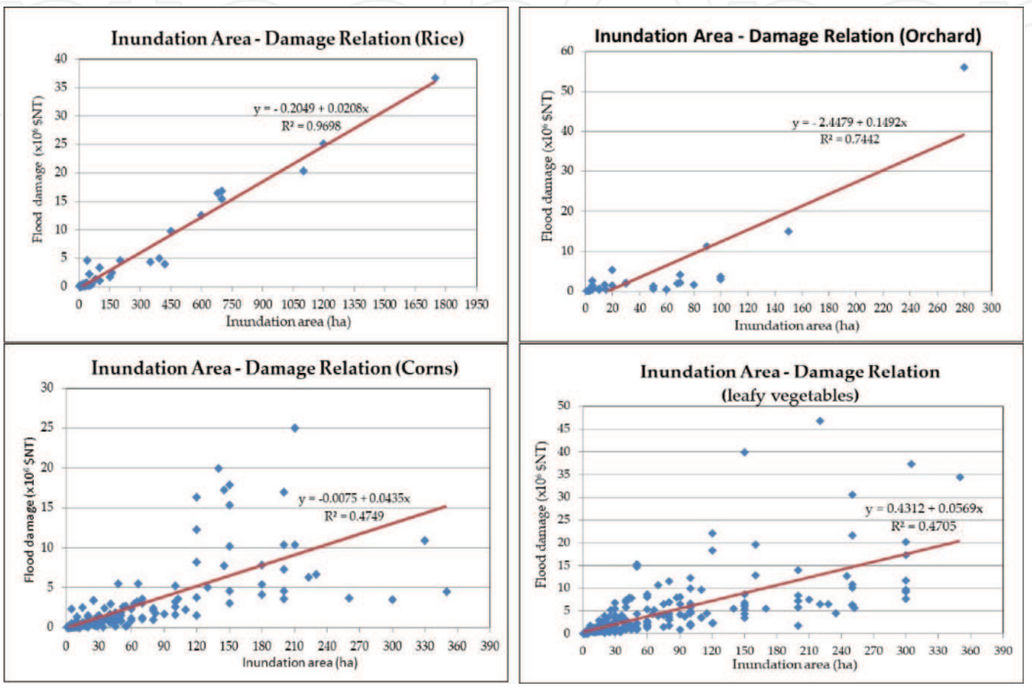

Figure 11.
Flood damage relationships for different agricultural produces.

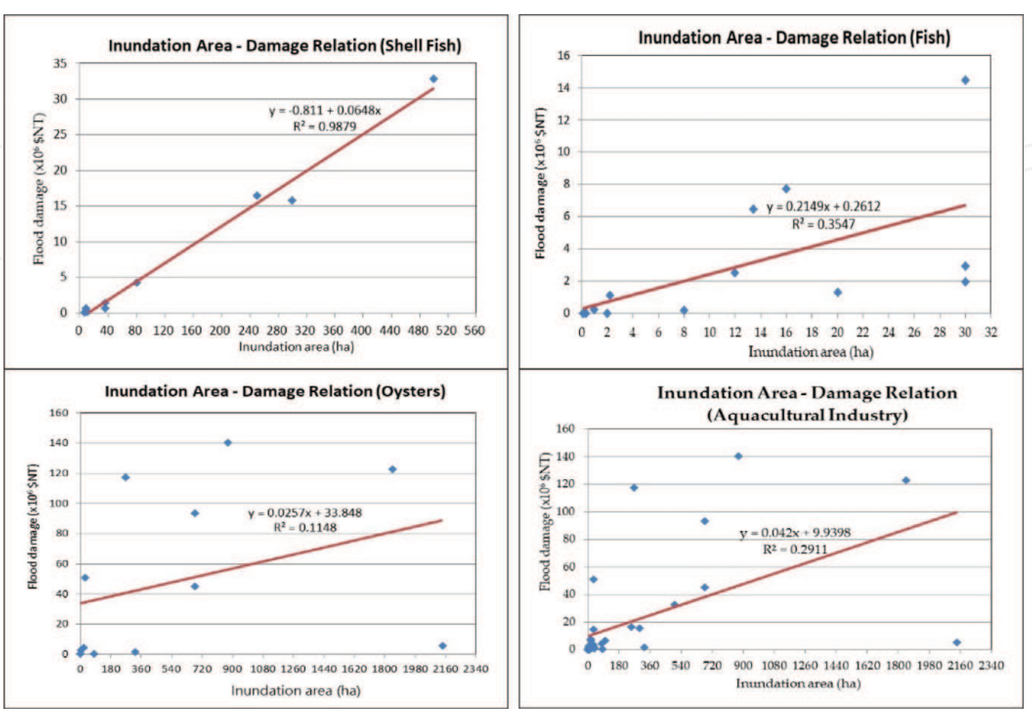

Figure 12.
Flood damage relationships for different aquacultural products.

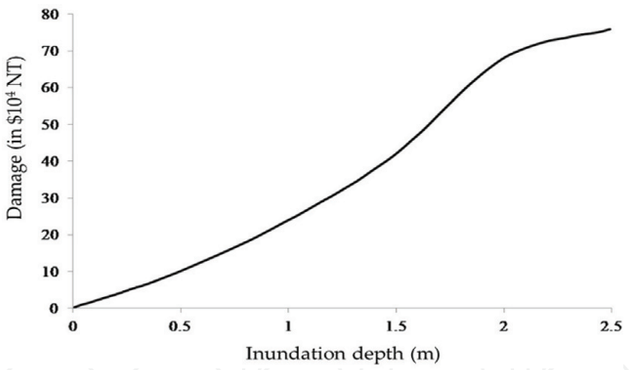

Figure 13.
Damage-inundation depth relationship for buildings in the study area.

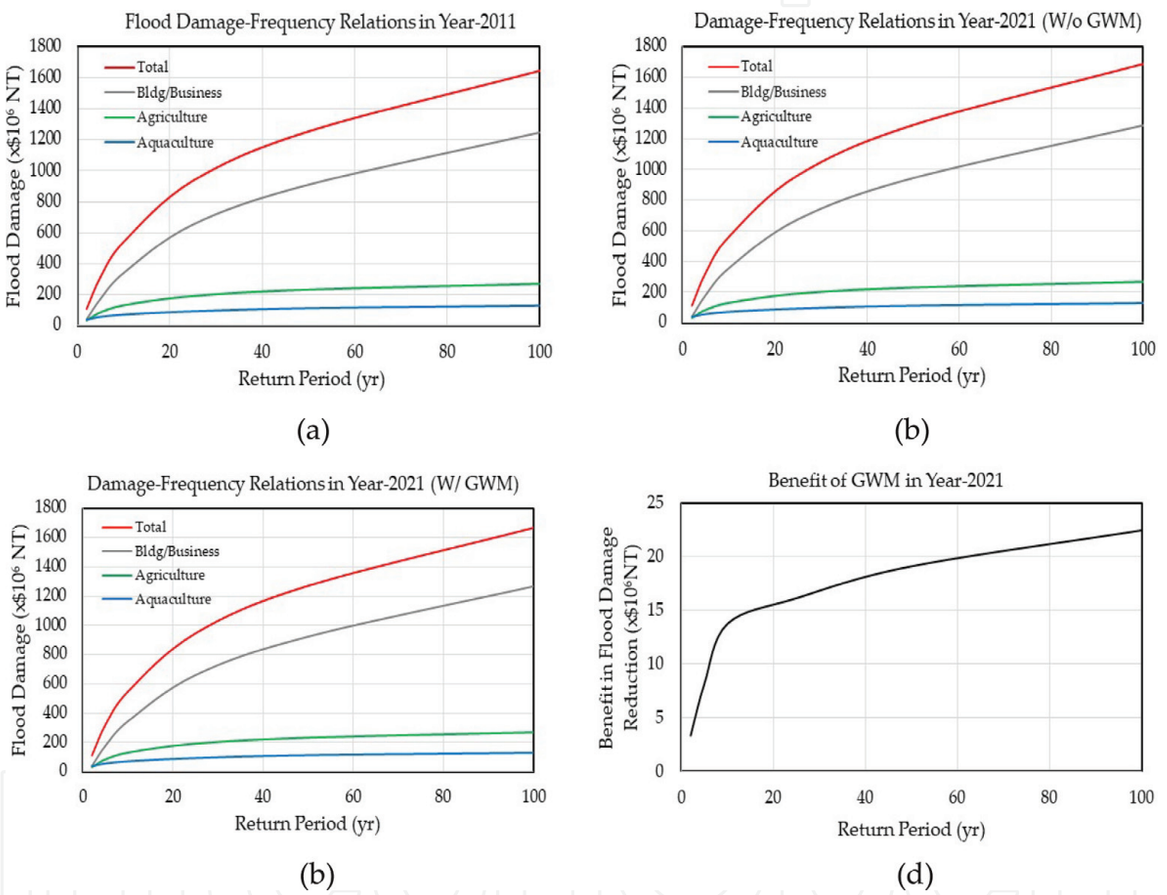

Figure 14.
Flood damage-frequency relationships under different scenarios. (a) In Year 2011. (b) In Year 2021 W/o GWM. (c) In Year 2021 W/ GWM. (d) Difference between w/o and w/ GWM.

rainstorm of different frequencies, areal extent and maximum water depth of inundation can be determined. These hydraulic modeling results, jointly with land use maps and inundation-damage relationships, allow the establishment of damage-frequency relationships as shown in **Figure 14(a)–(c)**. **Figure 14(a)** is derived according to Year 2011 land topography of the study area which serves as the initial condition for the 10-year GWM period. **Figure 14(b)** and **(c)**, respectively, is based on Year 2021 land topography as the consequence of with and without implementing GWM. To assess the economic merit of implementing GWM, the benefit due to inundation damage reduction in Year 2021 can be obtained as the difference between inundation damage with and without GWM, that is,

$$B(T|2021) = InunDmg(T, w/o\ GWM|\ 2021) - InunDmg(T, w/GWM|\ 2021) \quad (8)$$

in which $B(T|2021)$ = benefit of GWM (in terms of inundation damage reduction) in Year 2021 under a T-year rainstorm; $InunDmg(T, w/GWM|2021)$ and $InunDmg(T, w/o\ GWM|2021)$ = inundation damage in the study area with and without GWM, respectively, while subject to the T-year rainstorm. Based on **Figure 14(b)** and **(c)**, one can obtain **Figure 14(d)** showing the benefit-frequency relationship for implementing GWM in Year 2021. Then, the annual expected benefit by GWM in Year 2021 can be calculated by

$$E(B|2021) = \int_1^\infty B(T|2021)\left(\frac{1}{T^2}\right) dT \quad (9)$$

where $E(B|2021)$ = annual expected benefit of GWM for the year at the end of the 10-year management period 2012–2021. Note that land subsidence is a continuous process that progresses over the GWM period. It is anticipated that, from the initiation of GWM in Year 2012, the task will begin to accrue flood damage reduction (FDR) benefit over each individual management year with an increasing rate. The present worth of cumulative expected FDR benefit over the 10-year management period can be obtained as

$$PW(EB) = \sum_{t=2012}^{2021} E(B|t) \times \left(\frac{1}{1+i}\right)^{t-2011} \quad (10)$$

in which $PW(EB)$ = present worth of cumulative expected FDR benefit; $E(B|t)$ = expected FDR benefit by GWM for Year-t; and i = interest rate. The term $E(B|t)$ can be evaluated by Eqs. (8) and (9) for each individual year according to the flood inundation simulation results using the estimated land surface topography under the condition of with and without GWM. This would require hydraulic inundation simulation for each individual year, and the computation effort could be quite extensive.

To simplify the computation for economic merit assessment, it is assumed that the yearly FDR benefit increases linearly from zero in 2011 to $E(B|2021)$ over a 10-year management period. That is, annual expected FDR benefit increases at an annual rate of $E(B|2021)/10$. With this discrete uniform gradient cash flow pattern, the present value of the total expected FDR benefit accrued over the 10-year management period, $PW(EB)$, can be computed as

$$PW(EB) = \left(\frac{E(B|2021)}{10}\right) \times UGPV(n, i) \quad (11)$$

where $UGPW(n, i)$ = uniform gradient present worth factor, which can be computed by [19]:

$$UGPW(n, i) = \frac{(1+i)^n - (1+ni)}{i^2(1+i)^n} \quad (12)$$

in which n = length of management period, that is, n = 10 in this application.

According to the total inundation damage-frequency relationships shown in **Figure 14(a)–(c)** and Eq. (9), the estimated annual expected inundation damages for Year 2011, Year 2021 (w/o GWM), and Year 2021 (w/GWM) are 213.695, 223.527, and 218.406 M$NT(million New Taiwan dollars), respectively. Therefore, the incremental inundation damage in Year 2021 due to pumping-induced land

subsidence over a 10-year management period of with and without GWM are, respectively, 9.833 and 4.712 M$NT. The benefit of GWM in Year 2021 associated with the expected FDR in the study area is $E(B|2021) = 9.833 - 4.712 = 5.121$ M$NT. Assume that the interest rate is 4.5% and the annual expected benefit by GWM follows a linear increasing pattern from 0 (in Year 2011) to 5.121 M$NT (by Year 2021), the value of the uniform gradient present worth factor in Eq. (12) is $UGPW(n = 10, i = 4.5\%) = 32.74$. The corresponding present worth of the total benefit by GWM accrued in the study area over the 10-year GWM, by Eq. (11), is 16.768 M$NT or equivalent to an annual benefit of 2.119 M$NT amortized in 10 years.

By comparing the total amount of inundation damage amount in the study area (in the order of 200 M$NT annually), the GWM benefit associated with FDR does not appear to be very impressive. This might be due to a relatively short management period of 10 years. For sustainable GWM, the period of management would generally be longer and it can be easily shown, by a similar analysis described above, that the economic benefit of GWM in terms of flood damage reduction would grow with the management period. Furthermore, **Figure 8** clearly shows that implementing GWM in the land subsidence prone area can sustain the design flood protection level of drainage systems by preventing the freeboard from decreasing. This implies that potential huge saving in the capital cost can be realized because the lower levee height in many parts of the study area would be sufficient if an effective GWM policy is in the place. Also, the maintenance cost for levee systems could be reduced as fewer existing levee segments require height upgrading because the mandated freeboard can be upheld or even improved by GWM.

4. Conclusions

Groundwater is an important source of water supply, especially in regions where surface water supply is insufficient or not stable. However, the lack of proper management for groundwater extraction and usage in land subsidence prone areas could create a number of undesirable consequences such as damaging building structures, aggravating flood inundation hazards, and diminishing effectiveness of flood control facilities. This chapter presents a methodological framework demonstrating how a subsidence-focused GWM model can be formulated and applied to obtain an optimal pumping strategy that reduces the negative impact of land subsidence in a coastal region in western Taiwan which is experiencing serious land subsidence and associated flood hazards. Numerical results clearly show that, through the use of an optimal GWM model with an explicit consideration given to subsidence control, one is able to ease off uneven land surfaces and reduce seriousness of land subsidence and flood damage as well as sustain the flood protection level of drainage systems by maintaining a suitable freeboard. All these features provide strong evidence that GWM can play an important role, along with other engineering measures, in providing a sustainable solution to flood inundation problem in land subsidence prone areas.

Acknowledgements

This study was support by the Water Resources Planning Institute, Water Resources Agency, Ministry of Economic Affairs of Taiwan.

Conflict of interest

No potential conflict of interest is present in this chapter.

Nomenclature

B	layer thickness
$E(B\|t)$	expected FDR benefit by GWM in Year-t
g	gravitation acceleration
i	interest rate
$InunDmg(T, w/GWM\|t)$	inundation damage in the study area with GWM while subject to the T-year rainstorm
$InunDmg(T, w/o\ GWM\|t)$	inundation damage without GWM while subject to the T-year rainstorm
k_{uc}	the kuc-th control point outside the near-shore low-lying area
k_c	the kc-th control point within the near-shore low-lying area
NC	number of control points inside near-shore low-lying area
NL	number of layers in groundwater aquifer
NP	number of pumping wells
NT	number of groundwater management period
NUC	number of control points outside near-shore low-lying area
$Q(j,t)$	pumping rate at the j-th well during the t-th time period
$Q_D(t)$	groundwater demand during the t-th time period
$Q^L(j,t)$	minimum pumping rates at the j-th well during the t-th time period
$Q^U(j,t)$	maximum allowable pumping rates at the j-th well during the t-th time period
$UGPW(\bullet)$	uniform gradient present worth factor
α	the ratio of elastic to inelastic compaction per unit increase in drawdown
$\Delta s_{l,k,t}$	land subsidence within layer-l at point-k during the t-th time period
$\Delta h_{l,k,t}$	drawdowns of layer-l, point-k at the end of the t-th time period
ρ_w	density of water
$\Delta h^p_{l,k,t}$	difference between initial head and preconsolidation head at the end of the t-th time period
$\Delta s(\bullet)$	cumulated land subsidence at control points at the end of the management period
$\Delta s^*(\bullet)$	maximum allowable land subsidence at control points at the end of the management period
μ, λ	Lame constants

Author details

Yin-Lung Chang[1], Jinn-Chuang Yang[1], Yeou-Koung Tung[1*], Che-Hao Chang[2] and Tung-Lin Tsai[3]

1 Disaster Prevention and Water Environment Research Center, National Chiao-Tung University, Hsinchu, Taiwan

2 Department of Civil Engineering, National Taipei University of Technology, Taipei, Taiwan

3 Department of Civil and Water Resources Engineering, National Chiayi University, Chiayi, Taiwan

*Address all correspondence to: yk2013tung@gmail.com

References

[1] Phien-wej N, Giao PH, Nutalaya P. Land subsidence in Bangkok, Thailand. Engineering Geology. 2006;**82**(4): 187-201

[2] Nicholls RJ, Hanson S, Herweijer C, Patmore N, Hallegatte S, Corfee-Morlot J. Ranking port cities with high exposure and vulnerability to climate extremes: Exposure estimates. In: OECD Environment Working Papers, No. 1. OECD Publishing; 2008

[3] Marfai MA, King L. Tidal inundation mapping under enhanced land subsidence in Semarang, Central Java Indonesia. Natural Hazards. 2008; **44**(1):93-109

[4] Ward PJ, Marfai MA, Yulianto F, Hizbaron DR, Aerts JCJH. Coastal inundation and damage exposure estimation: A case study for Jakarta. Natural Hazards. 2011;**56**(3):899-916

[5] Wang J, Gao W, Xu SY, Yu LZ. Evaluation of the combined risk of sea level rise, land subsidence, and storm surges on the coastal areas of Shanghai, China. Climatic Change. 2012;**115**(3–4): 537-558

[6] Gambolati G, Teatini P, Gonella M. GIS simulations of the inundation risk in the coastal lowlands of the Northern Adriatic Sea. Mathematical and Computer Modelling. 2002;**35**(9–10): 963-972

[7] Freeze RA, Gorelick SM. Convergence of stochastic optimization and decision analysis in the engineering design of aquifer remediation. Ground Water. 1999;**37**(6):934-954

[8] Gorelick SM. A review of distributed parameter groundwater management modeling methods. Water Resources Research. 1983;**19**(2):305-319

[9] Gorelick SM, Zheng C. Global change and the groundwater management challenge. Water Resources Research. 2015;**51**(5):3031-3051

[10] Phillips SP, Carlson CS, Metzger LF, Howle JF, Galloway DL, Sneed M, Ikehara ME, Hudnut KW, King NE. Analysis of tests of subsurface injection, storage, and recovery of freshwater in Lancaster, Antelope Valley, California. U.S. Geological Survey Water-Resources Investigations Report 03-4061. 2003. pp. 93-100

[11] Chang YL, Tsai TL, Yang JC, Tung YK. Stochastically optimal groundwater management considering land subsidence. Journal of Water Resources Planning and Management. 2007; **133**(6):486-498

[12] Chang YL, Huang CY, Tsai TL, Chen HE, Yang JC. Optimal groundwater quantity management for land subsidence control. In: Proceedings of the IASTED International Conference on Environmental Management and Engineering, 4-6 July 2011; Calgary, A. B., Canada. pp. 38-45

[13] Chang YL. The influence of hydrologic and topographic uncertainties on inundation risk in Sourthwest coastal area. Water Resources Planning Institute, Water Resources Agency, Ministry of Economic Affairs, Taiwan. Report: MOEAWRA1020238. 2013 (in Chinese)

[14] Deltares. SOBEK, User Manual. Delft, The Netherlands: Deltares; 2014

[15] WRPI. Handbook for Planning of Regulation and Environment Rehabilitation of Drainage System. Taiwan: Water Resources Planning Institute, Water Resources Agency; 2006. (in Chinese)

[16] Chow VT. Open Channel Hydraulics. McGraw-Hill; 1959

[17] Tsai TL. The development and application of model of regional land subsidence due to groundwater overpumping [thesis]. Hsinchu, Taiwan: National Chiao Tung University; 2001. (in Chinese)

[18] Leake SA. Interbed storage changes and compaction in models of regional groundwater-flow. Water Resources Research. 1990;**26**(9):1939-1950

[19] Park CS, Sharp-Bette GP. Advanced Engineering Economics. Wiley; 1990. p. 740